

# CO<sub>2</sub> sequestration in the Frio Fm., TX: Evaluation of the impact of CO<sub>2</sub>, co-contaminant gas, aqueous fluid and reservoir rock interactions

Kevin G. Knauss, James W. Johnson and Carl I. Steefel  
Lawrence Livermore National Laboratory

## Abstract

Lowering the costs of front-end processes (e.g., separation) in the geologic sequestration of CO<sub>2</sub> can dramatically lower the overall costs. One approach is to sequester less-pure CO<sub>2</sub> waste streams that are less expensive or require less energy to separate from flue gas, a coal gasification process, etc. The objective of this research is to evaluate the impacts of CO<sub>2</sub> itself, as well as an impure CO<sub>2</sub> waste stream, on geologic sequestration using reaction progress models, reactive transport simulators and analogous reactive transport experiments run in a plug flow reactor. Specifically, we are investigating the potential for co-injecting SO<sub>x</sub>, NO<sub>x</sub>, and H<sub>2</sub>S present in coal-fired waste streams along with CO<sub>2</sub>.

Coupling a chemical model with simplified fluid flow using the reactive transport code CRUNCH (Steefel, 2001), we have simulated the results of injection into a heterogeneous rock formation and have accounted for mineralogical changes along the flow path. To simulate conditions associated with a long term sequestration effort, we continued the injection phase for 5y under a radial flow field and then instantaneously switched to a much slower linear flow field of the starting composition reservoir fluid (i.e., acid gas free) for an additional 95y. The impact of the various gases is then compared.

As a first step in the validation of the reactive transport simulator, we have conducted a plug flow reactor experiment designed specifically to test simultaneous primary mineral dissolution and secondary mineral growth.

## Model Definition

Our model was constructed using reservoir fluid and rock data from wells completed in the Frio Fm. in Texas. This unit is the proposed site for a CO<sub>2</sub> sequestration pilot project (Hovorka et al., 2002). Mineral specific surface areas were calculated assuming 200 μ grains. Because the fluid analyses were incomplete (they failed to analyze for K, Al, Si or O<sub>2</sub>), as a starting point for the reservoir fluid composition we assumed that these missing elements were controlled by mineral equilibria (illite, kaolinite, quartz and pyrite, respectively) and then used CRUNCH to react a very slowly moving reservoir fluid with the rock sufficiently long (2000 years) that an essentially steady-state fluid composition was achieved. This calculation also allowed us to estimate the secondary minerals that could potentially form in this system (anhydrite, barite, chalcedony, dawsonite, magnesite, siderite and strontianite).

Reservoir Rock				Reservoir Fluid	
Mineral	Mode (vol %)	SSA (m <sup>2</sup> /g)	Edge factor	Species (basis)	Concentration (molality)
Quartz	60.06	0.01133		Al+++	3.2234E-08
K-feldspar	4.26	0.01173		Ba++	4.3092E-04
Illite/muscovite	0.96	0.01060	10x	Sr++	1.2490E-03
Calcite	0.71	0.01107		Ca++	5.5291e-02
Kaolinite	0.66	0.01156	10x	CO <sub>2</sub> (aq)	1.0097E-03
Chlorite/clinochlore	0.51	0.01118	10x	Fe++	6.4972E-04
Labradorite	2.48	0.01087		K+	1.0594e-02
Pyrite	0.35	0.00599		Mg++	1.9001e-02
				Na+	1.7767E+00
				SiO <sub>2</sub> (aq)	4.0135E-04
				Cl-	1.9394E+00
				SO <sub>4</sub> --	1.0746E-04
				O <sub>2</sub> (aq)	4.8417e-63

## Simulation Conditions

We set up a simple 1D, radially symmetric simulation using an analytical expression to calculate a radial Darcy flow field that closely approximates the flow field (and resulting observation well breakthrough time) that was generated from 3D TOUGH2 (Pruess, 2002) transport-only modeling of CO<sub>2</sub> injection into the Frio sand (Doughty, 2002). The expression we used is:

$$V(x) = Q/(2\pi x h \phi S_g \rho)$$

where:  $V(x)$  = Darcy flux at  $x$ ,  $x$  = radial distance,  $Q$  = CO<sub>2</sub> injection rate (250T/d),  $h$  = cylinder height of injection interval,  $\phi$  = porosity (30%),  $S_g$  = residual gas saturation behind front (0.55), and  $\rho$  = density of CO<sub>2</sub> at T&P (565 kg/m<sup>3</sup> at 64°C and 150b total CO<sub>2</sub> pressure). Under injection conditions the CO<sub>2</sub> fugacity is 84.3b.

Because our primary interest is in the rock/water interaction arising from acid created by dissolving CO<sub>2</sub> and other waste gases, we simplified the simulation by injecting the volume equivalent amount of reservoir fluid equilibrated with the appropriate waste gas fugacities. In the CO<sub>2</sub> only case, this is 84.3b; for the CO<sub>2</sub> + H<sub>2</sub>S case we added 10b of H<sub>2</sub>S; and for the CO<sub>2</sub> + SO<sub>2</sub> case we added 10<sup>-6</sup>b of SO<sub>2</sub>. In order to track the CO<sub>2</sub> front, we included a tracer (fictitious, perfectly conservative species) in the simulation.

To simulate conditions associated with a long term sequestration effort, we continued the injection phase for 5y under the radial flow field and then instantaneously switched to a much slower linear flow field (a Darcy flow of 0.15m/y) of the starting composition reservoir fluid (i.e., acid gas free). This would approximate the return to regional flow after injection stops and these conditions were simulated for an additional 95y.

## Chemical Kinetics and Thermodynamics

Because the reservoir fluids become so acidic, we use kinetic rate laws that explicitly account for acid catalysis of mineral dissolution. The kinetic rate law and Arrhenius expression used to extrapolate rate constants in temperature are shown below. The thermodynamic data used are largely from the SUPCRT database (Johnson et al., 1992).

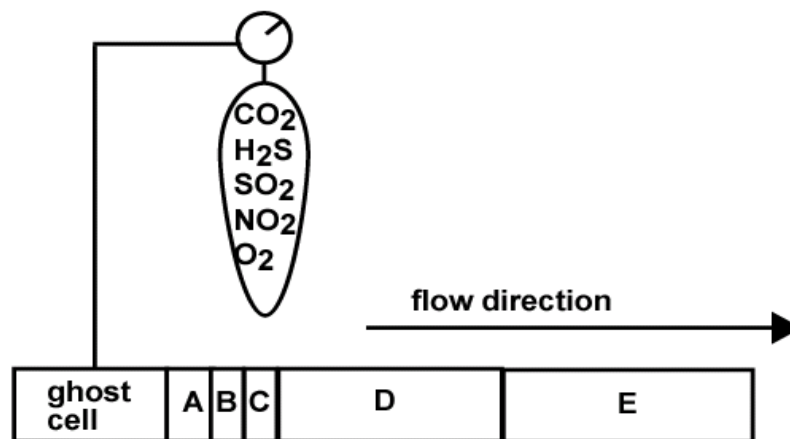
$$r_m = k_m A_m \prod_{i=1}^N a_i^n \left( \frac{Q}{K} \right) - 1 \quad k_m = k_{m,T_r} \exp \left[ \frac{-E_a}{R} \left( \frac{1}{T} - \frac{1}{T_r} \right) \right]$$

### Kinetic Parameters

mineral	log k (mol/m <sup>2</sup> *s)	E <sub>a</sub> (kcal)	n	source
Albite	-9.69	14.3	.5	Blum & Stillings (1995)
Albite	-12.0	16.2	0	Blum & Stillings (1995)
Anhydrite	-2.76	7.65	.11	Barton & Wilde (1971); Dove & Czank (1995)
Labradorite	-8.86	15.9	.5	Blum & Stillings (1995)
Labradorite	-12.0	16.2	0	Assume similar to albite
Barite	-7.19	7.65	.11	Dove & Czank (1995)
Calcite	-1.16	4.54	1.0	Alkattan et al. (1998)
Calcite	-6.19	15.0	0	Chou et al. (1989)
Chalcedony	-12.7	16.5	0	Rimstidt & Barnes (1980) - α-cristobalite
Clinocllore	-11.6	15.0	0	Malmstrom et al. (1996)
Dawsonite	-7.00	15.0	0	Assume between calcite and magnesite
K-feldspar	-9.45	12.4	.4	Blum & Stillings (1995)
K-feldspar	-12.0	13.8	0	Blum & Stillings (1995)
Kaolinite	-11.6	15.0	.17	Nagy (1995)
Kaolinite	-13.0	15.0	0	Nagy (1995)
Magnesite	-4.36	4.54	1.0	Chou et al. (1989)
Magnesite	-9.35	15.0	0	Chou et al. (1989)
Muscovite	-11.7	5.26	.4	Knauss & Wolery (1989); Nagy (1995)
Muscovite	-13.0	15.0	0	Knauss & Wolery (1989); Nagy (1995)
Pyrite	-8.00	15.0	0	Steeffel (2001)
Quartz	-13.9	20.9	0	Testor et al. (1994)
Siderite	-3.01	5.00	.9	Gautelier et al. (1999) - dolomite
Siderite	-8.90	15.0	0	Steeffel (2001)
Strontianite	-3.03	10.0	1	Sonderegger (1976)
Strontianite	-7.35	10.0	0	Sonderegger (1976)

## Simulation Schematic

We simulated the reactive transport over a 1km domain with 164 cells progressing in size from 1m between the injection well and an observation well located 30 m away to 10m further out into the domain.



**ghost cell:**  
formation fluid  
CO<sub>2</sub> = 84.3b  
O<sub>2</sub> ~ 10<sup>-60</sup>b  
no minerals

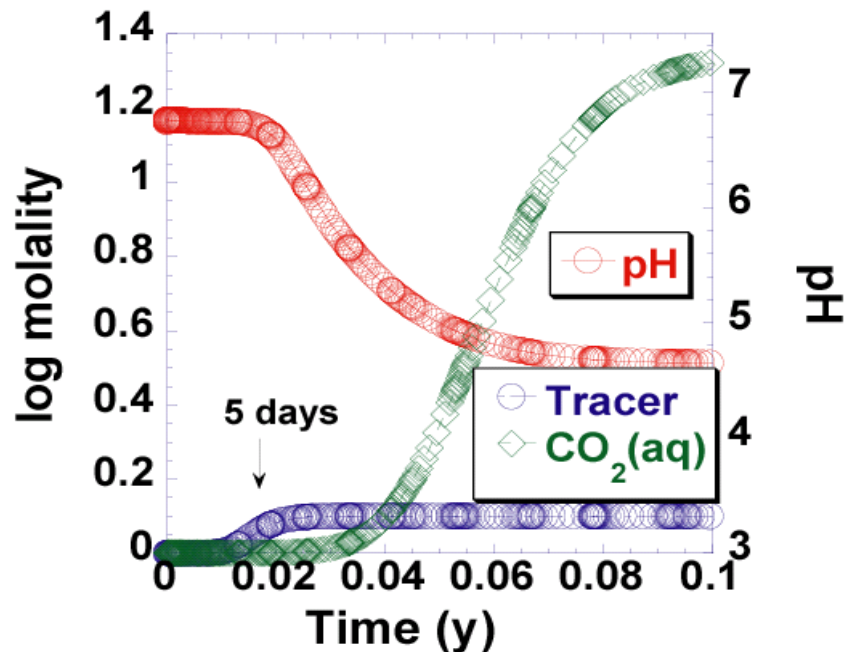
A = 30 x 1 m  
B = 10 x 2 m  
C = 5 x 4 m  
D = 52 x 5 m  
E = 67 x 10 m

**initial condition:**  
formation fluid  
O<sub>2</sub> ~ 10<sup>-60</sup>b  
"equilibrate" with  
Quartz  
K-Feldspar  
Labradorite  
Illite  
Calcite  
Kaolinite  
Clinochlore  
Pyrite

## Breakthrough at Observation Well

Below we show the simulated breakthrough curves at the location of the observation well, as well as a table of relative change in water composition in the observation well. For comparison we also tabulate the relative change in water composition observed at a production well in the Rangely Field CO, just at breakthrough during a CO<sub>2</sub> flood (Bowker and Shuler, 1991). The results compare reasonably well with the exception of Fe and CO<sub>2</sub>, which are explained by contamination and sampling loss, respectively. The breakthrough time (~5d) agrees with that predicted from TOUGH2 hydrologic modeling.

### Observation Well (30m)

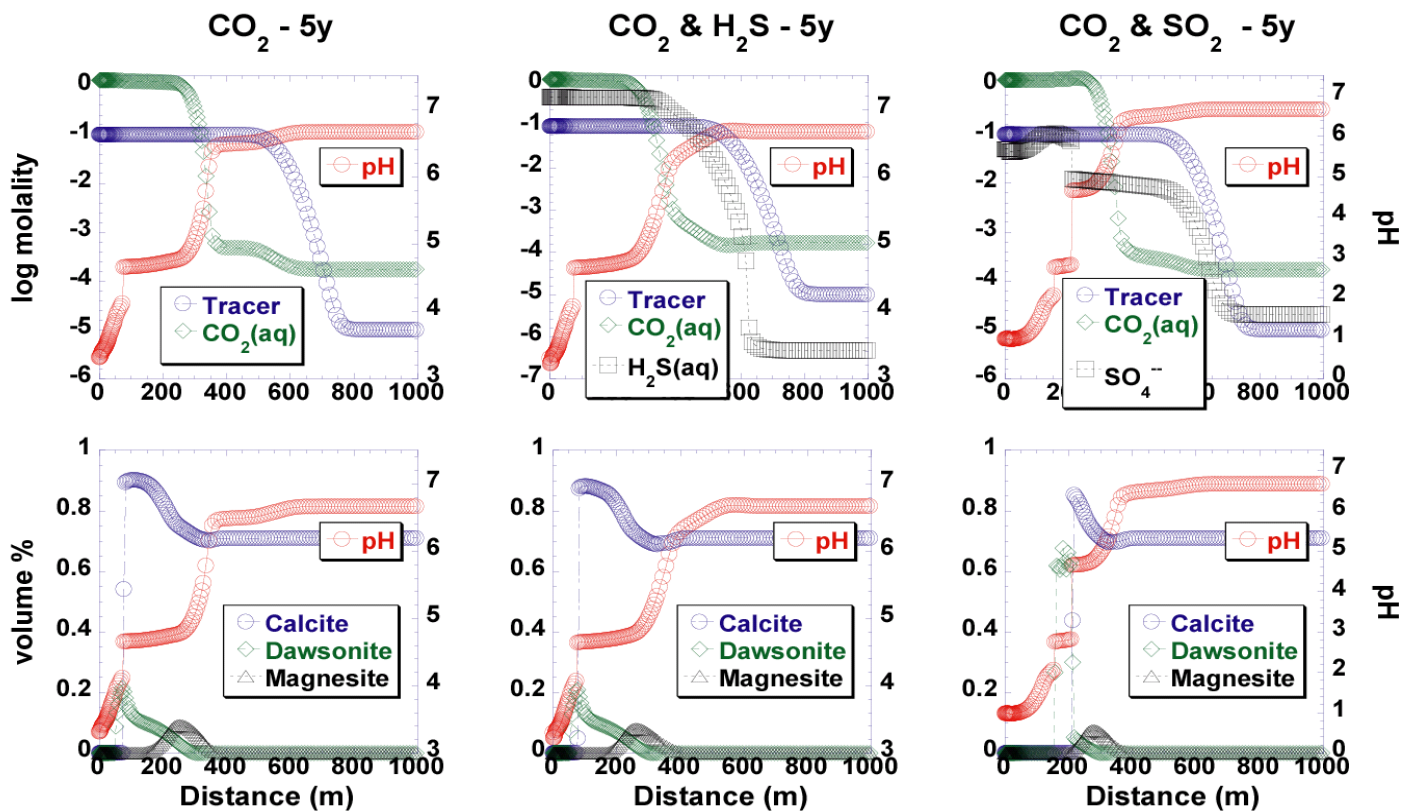


	Frio model	Rangely
pH	6.74 -> 4.65	6.5 -> 4.5
Ca <sup>++</sup>	+19%	+19%
Mg <sup>++</sup>	+7.4%	+29%
Fe <sup>++</sup>	nc (< 1%)	+816%
Ba <sup>++</sup>	nc	+5%
Sr <sup>++</sup>	nc	+21%
K <sup>+</sup>	+1.3%	+10%
HCO <sub>3</sub> <sup>-</sup>	+2560%	+128%

## Simulation Results - End of Injection

At the end of the injection period the tracer has progressed 750m into the domain, although the  $\text{CO}_2(\text{aq})$  front propagates at a slower velocity, due to rock/water interactions, etc. The incoming fluid has a pH of 3.2 (fixed by the  $\text{CO}_2$  fugacity), because all the calcite originally present has been consumed. There is no longer rapid pH buffering. Between about 75m - 300m the original calcite still remains to buffer the pH even in the presence of  $\text{CO}_2(\text{aq})$  and is actually growing, consuming the excess  $\text{Ca}^{+2}$  liberated upstream by dissolution of both calcite and labradorite where pH is low. The addition of  $\text{H}_2\text{S}$  to the waste stream doesn't have a tremendous effect on the rock/water interaction. The  $\text{SO}_2$ , however, does make a significant difference, due to the lower pH created. Note the different pH scale in this plot. By the end of injection the incoming fluid has a pH of 1. Also, the distribution of aqueous S-species differs markedly ( $\text{SO}_4^{--}$  vs.  $\text{H}_2\text{S}(\text{aq})$ ), owing to the formation of anhydrite over the first 200m of the domain in the case of  $\text{SO}_2$  injection.

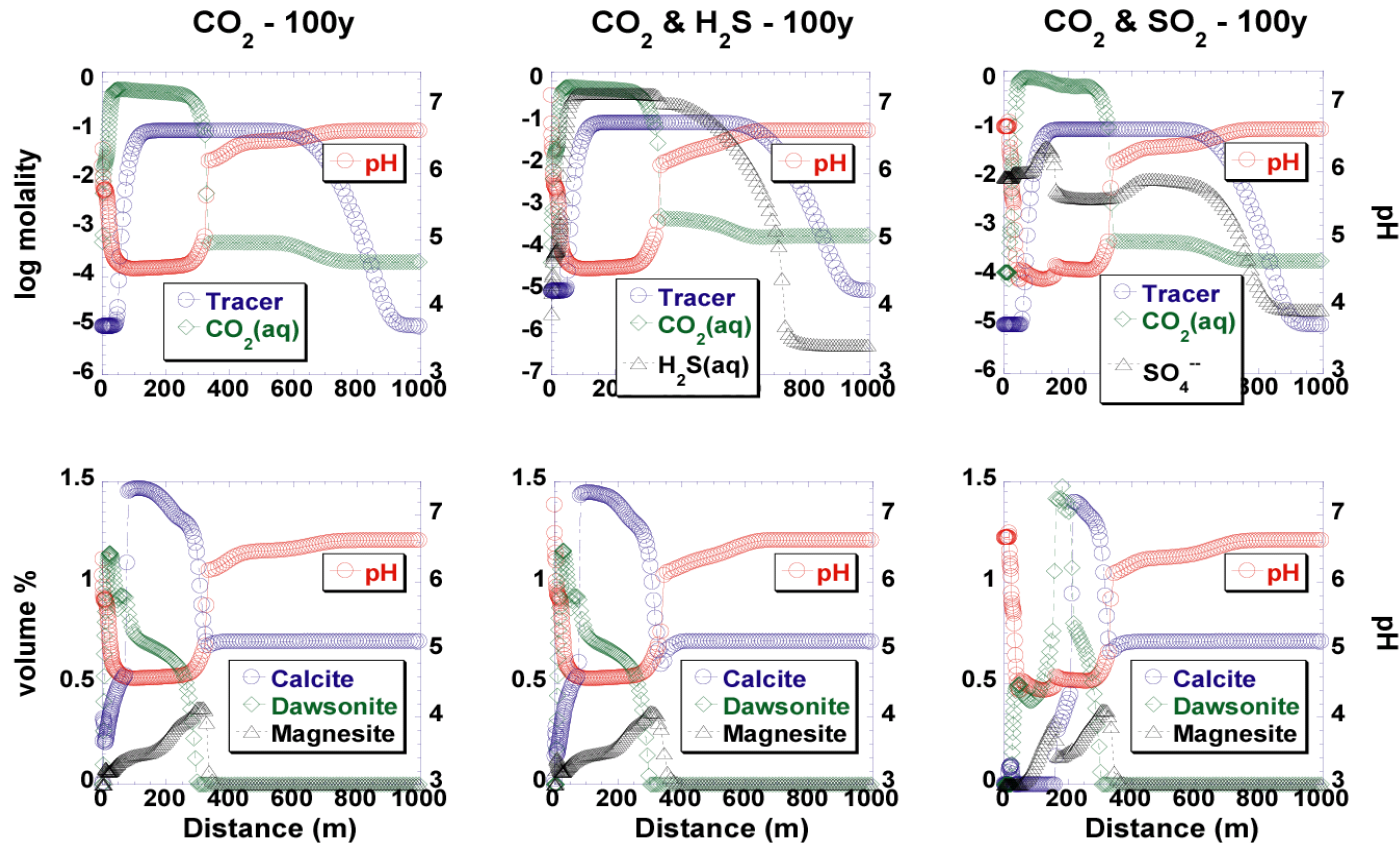
In all three cases carbonate minerals are forming. Although some of the calcite is simply being mobilized and moved downstream, where it can reprecipitate under favorable pH conditions, the formation of dawsonite and magnesite represent new C sinks. Note how the distribution of the carbonate minerals in space displays a chromatographic effect, reflecting the pH distribution, and mapping out the pH stability fields for each mineral.



## Simulation Results - 95 years later

After 95 years of flow under a simulated slow regional flow condition, based on the return of the tracer peak to the original starting reservoir fluid concentration, it is seen that flow has moved less than 50m in that time period. However, under these more stagnant flow conditions considerable changes in fluid chemistry and mineralogy have occurred. In all 3 cases the pH has risen everywhere throughout the domain, while the  $\text{CO}_2(\text{aq})$  curves have correspondingly decreased. This is due to rock/water interaction dominated by the dissolution of silicate minerals at low pH and the growth of carbonate minerals that consume the liberated metals. As pH increases above approximately 6.5, the aqueous C-speciation is also changing to be dominated by  $\text{HCO}_3^-$ , rather than  $\text{CO}_2(\text{aq})$ . The  $\text{H}_2\text{S}(\text{aq})$  distribution is only slightly changed, while  $\text{SO}_4^{--}$  is decreased more noticeably by continued formation of anhydrite.

All 3 carbonate minerals have continued to grow under the slow flow conditions following injection. In fact, the carbonate minerals will continue to grow for a long time period beyond the simulation that we have done.



## Simulation Conclusions

These preliminary simulations suggest that even relatively large amounts of co-injected  $\text{H}_2\text{S}$  should not prove problematic for a  $\text{CO}_2$  injection process. In the case of  $\text{SO}_2$ , if conditions allow the S to be oxidized, only minor amounts of this gas could be tolerated, owing to the extremely low pH generated. Potential for porosity loss due to the formation of anhydrite will need to be assessed.

It is important to emphasize here that more fully coupled simulations need to be conducted that allow explicit feedback between porosity/permeability changes and transport processes, as well as dealing explicitly with the transport of a separate  $\text{CO}_2$ -rich phase (Johnson et al., 2000). For example, in an actual  $\text{CO}_2$  injection process the bulk of the  $\text{CO}_2$  injected over the time frame of this simulation would still remain as the free phase. Dissolved  $\text{CO}_2$  would be a significant sink for C, while the amounts of carbonate mineral formed would be a smaller sink.

It is also critical that we conduct well designed reactive transport experiments to benchmark the simulators that we use. This is a serious deficiency in the work done to date. We are presently conducting plug flow reactor experiments that closely mimic conditions in a  $\text{CO}_2$  injection process, that may be used for this validation purpose.

## References

- Alkattan M., Oelkers E. H., Dandurand J.-L., and Schott J. (1998) An experimental study of calcite and limestone dissolution rates as a function of pH from -1 to 3 and temperature from 25 to 80°C. *Chem. Geol.* 151, 199-214.
- Barton A. F. M. and Wilde N. M. (1971) Dissolution rates of polycrystalline samples of gypsum and orthorhombic forms of calcium sulphate by a rotating disk method. *Trans. Faraday Society* 66, 764-768.
- Blum A. E. and Stillings L. L. (1995) Feldspar dissolution kinetics. In *Chemical weathering rates of silicate minerals*, Vol. 31 (ed. A. F. White and S. L. Brantley), pp. 291-351. Mineralogical Society of America.
- Bowker K. A. and Shuler P. J. (1991) Carbon dioxide sequestration and resultant alteration of the Weber Sandstone, Rangely Field, Colorado. *Am. Assoc. Petrol. Geol.* 75(9), 1489-1499.
- Chou L., Garrels R. M., and Wollast R. (1989) Comparative study of the kinetics and mechanisms of dissolution of carbonate minerals. *Chem. Geol.* 78, 269-282.
- Doughty C. (2002) personal communication.
- Dove P. M. and Czank C. A. (1995) Crystal-Chemical Controls on the Dissolution Kinetics of the Isostructural Sulfates - Celestite, Anglesite, and Barite. *Geochim Cosmochim Acta* 59(10), 1907-1915.
- Gautelier M., Oelkers E. H., and Schott J. (1999) An experimental study of dolomite dissolution rates as a function of pH from -0.5 to 5 and temperature from 25 to 80°C. *Chem. Geol.* 157, 13-26.
- Hovorka S. D., Knox P. R., Yeh J. S., Fouad K., and Sakurai S. (2002) Sequestration pilot site in the Texas Gulf Coast, USA. 2002 Geological Society of America National Meeting.
- Johnson J. W., Oelkers E. H., and Helgeson H. C. (1992) SUPCRT92: A software package for calculating the standard molal thermodynamic properties of minerals, gases, aqueous species, and reactions from 1 to 5000 bars and 0 to 1000 oC. *Computers and Geosci.* 18, 899-947.
- Johnson J. W., Knauss K. G., Glassley W. E., DeLoach L. D., and Tompson A. F. B. (1998) Reactive transport modeling of plug-flow reactor experiments: quartz and tuff dissolution at 240°C. *J. Hydrol.* 209(1-4), 81-111.
- Johnson J. W., Steefel C. I., Nitao J. J., and Knauss K. G. (2000) Reactive transport modeling of subsurface CO2 sequestration: Identification of optimal target reservoirs and evaluation of performance based on geochemical, hydrologic, and structural constraints. *Energex 2000*.
- Knauss K. G. and Wolery T. J. (1989) Muscovite dissolution kinetics as a function of pH and time at 70°C. *Geochim. Cosmochim. Acta* 53, 1493-1501.
- Malmstrom M., Banwart S., Lewenhagen J., Duro L., and Bruno J. (1996) The dissolution of biotite and chlorite at 25°C in the near-neutral pH region. *Contaminant Hydrology* 21, 201-213.
- Nagy K. L. (1995) Dissolution and precipitation kinetics of sheet silicates. In *Chemical Weathering Rates of Silicate Minerals*, Vol. 31 (ed. A. F. White and S. L. Brantley), pp. 173-233.
- Pruess K. (2002) Numerical simulation of multiphase tracer transport in fractured geothermal reservoirs. *Geothermics* 31(4), 475-499.
- Rimstidt J. D. and Barnes H. L. (1980) The kinetics of silica-water reactions. *Geochimica et Cosmochimica Acta* 44(11), 1683-1699.
- Sonderegger J. L., Brower K. R., and Lefebvre V. G. (1976) A preliminary investigation of strontianite dissolution kinetics. *Am. J. Sci.* 276, 997-1022.
- Steefel C. I. (2001) CRUNCH, pp. 76. Lawrence Livermore National Laboratory.
- Testor J. W., Worley W. G., Robinson B. A., Grigsby C. O., and Feerer J. L. (1994) Correlating quartz dissolution kinetics in pure water from 25 to 625°C. *Geochim. Cosmochim. Acta* 58, 2407-2420.